Electronic Supplementary Material (ESI) for

Ir(III) complex–based phosphorescence and electrochemiluminescence chemodosimetric probes for Hg(II) ion with high selectivity and sensitivity

Hayoung Rhee, Taemin Kim, and Jong–In Hong*

Department of Chemistry, Seoul National University, 1 Gwanak–ro, Gwanak–gu, Seoul 08826, Korea
E–mail: jihong@snu.ac.kr

Table of Contents

X–ray Diffraction Studies

Experimental

Single crystals ($C_{26}H_{22}IrN_4$ [$(ppy)_2Ir(CH_3CN)_2$]) for X-ray diffraction were obtained by vapor diffusion of water into a concentrated solution of **2** in the presence of 0.5 equivalent of $Hg(NO_3)_2$ in acetonitrile. A suitable crystal was selected onto a nylon loop with Paratone® N oil and mounted on Agilent SuperNova, Dual, Cu at home/near, AtlasS2 diffractometer. The crystal was kept at 293.0(4) K during data collection using Cu Kα radiation (λ= 1.542 Å). A total number of 10459 reflections were measured (6.078° ≤ 2Θ ≤ 147.946°) with 1° steps (ω scan). The structure was solved with *ShelXT* software using direct methods and refined using least squares minimization refinement package of OLEX2. CCDC 1576742 contains the supplementary crystallographic data of this paper. These data can be obtained free of charge from the Cambridge Crystallographic Data Centre via www.ccdc.cam.ac.uk/data_request/cif.

Table S1. Crystallographic data and structure refinement information for $(ppy)_2Ir(CH_3CN)_2$.

Identification code	$(ppy)_2Ir(CH_3CN)_2$
Empirical formula	$C_{26}H_{22}IrN_4$
Formula weight	582.67
Temperature/K	293.0(4)
Crystal system	monoclinic
Space group	$P2_1/c$
a/Å	14.9543(4)
b/Å	20.0441(5)
c/Å	9.0693(2)
α/°	90
β/°	103.535(3)
γ/°	90
Volume/Å^3	2642.98(12)
Z	4
ρ_{calc}/g/cm^3	1.464
μ/mm^{-1}	9.905
F(000)	1132
Crystal size/mm^3	0.1 × 0.05 × 0.05
Radiation	CuKα (λ = 1.54184)
2Θ range for data collection/°	6.078 to 147.946
Index ranges	$-18 \le h \le 18$, $-20 \le k \le 24$, $-11 \le l \le 7$
Reflections collected	10459
Independent reflections	5203 [R_{int} = 0.0220, R_{sigma} = 0.0253]
Data/restraints/parameters	5203/0/258
Goodness–of–fit on F^2	1.07
Final R indexes [I≥2σ (I)]	R_1 = 0.0346, wR_2 = 0.0949
Final R indexes [all data]	R_1 = 0.0385, wR_2 = 0.0977

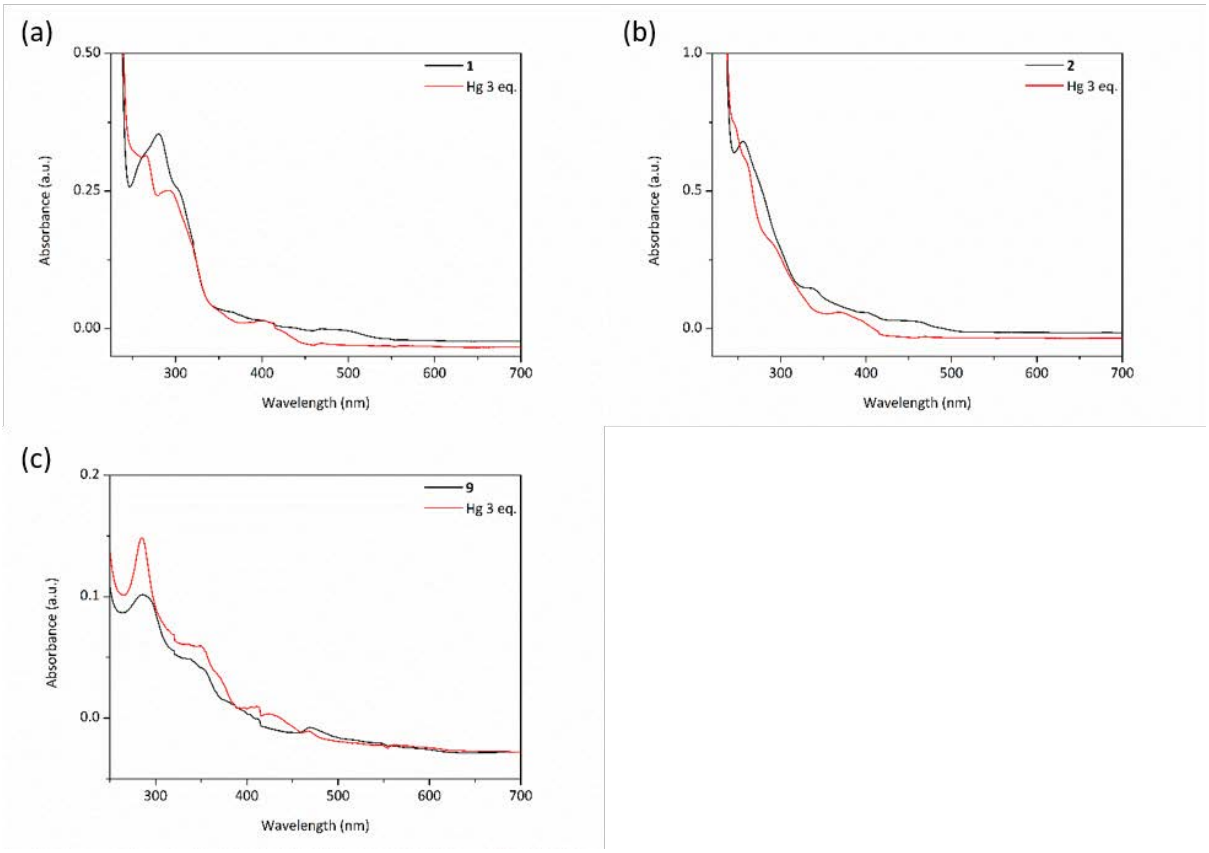

Figure S1. Changes in the absorption spectra of (a) **1**, (b) **2**, and (c) **9** in CH_3CN/water (9/1) upon the addition of 3 equivalents of Hg^{2+} ion.

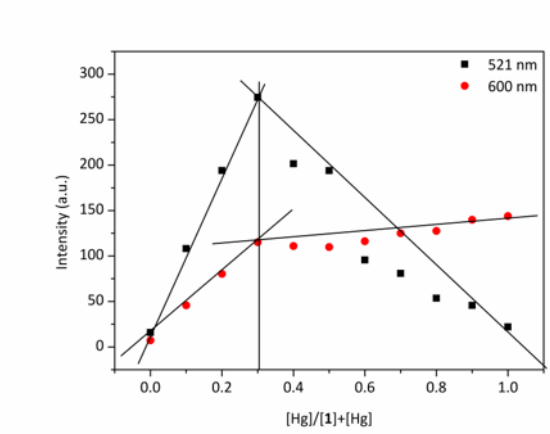

Figure S2. Job's plot for **1** and Hg^{2+} ion at 521 nm and 600 nm in CH_3CN/water (9/1).

[**1**] + [Hg^{2+}] = 5.0 x 10^{-5} mol L^{-1}. λ_{ex} = 400 nm.

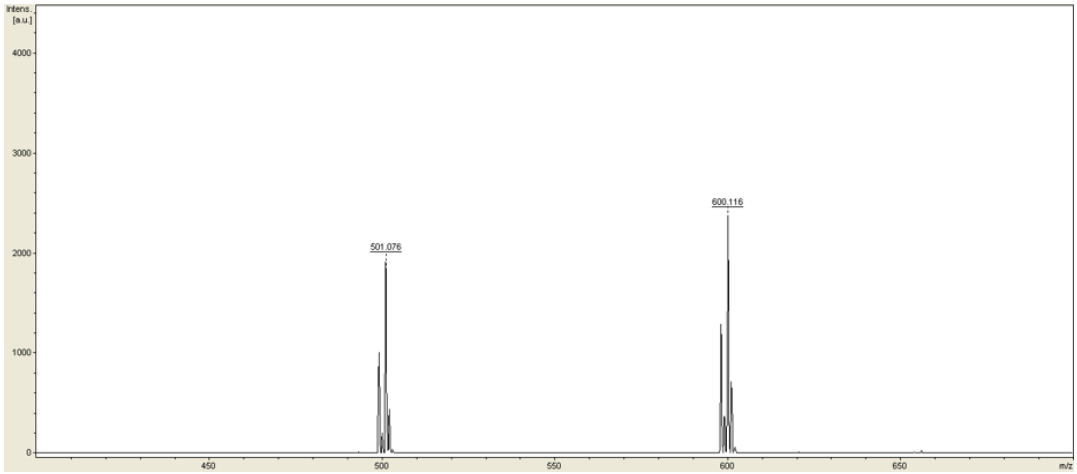

Figure S3. MALDI–TOF data of **2**.

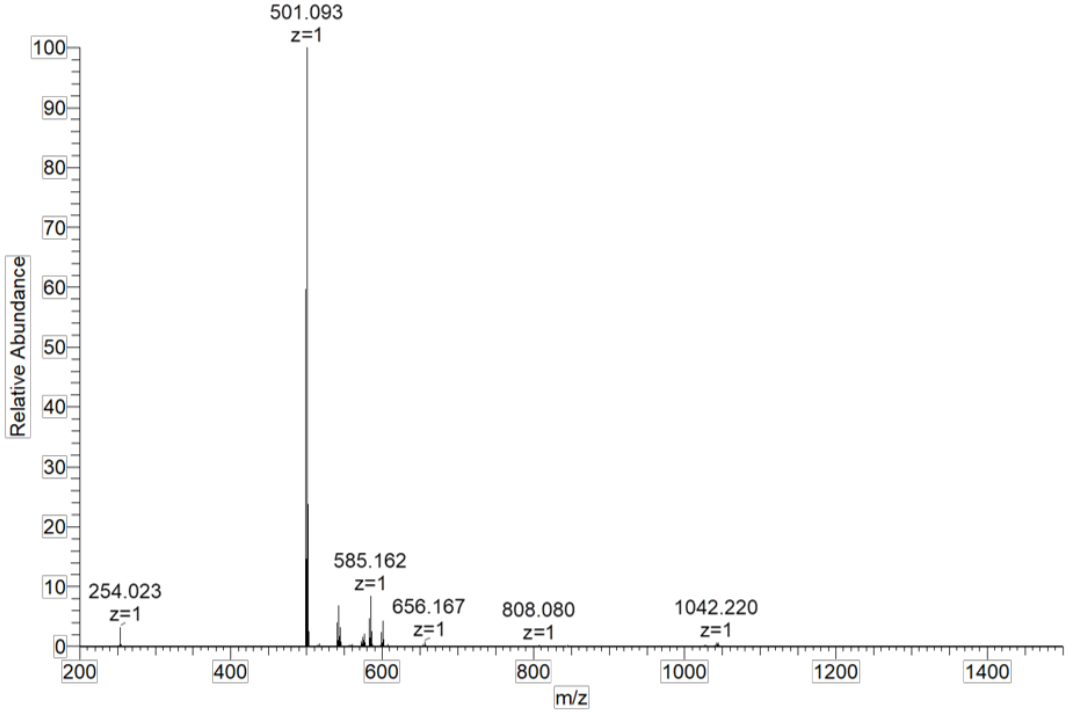

Figure S4. ESI–MS spectra of **2** after the addition of Hg^{2+} ion.

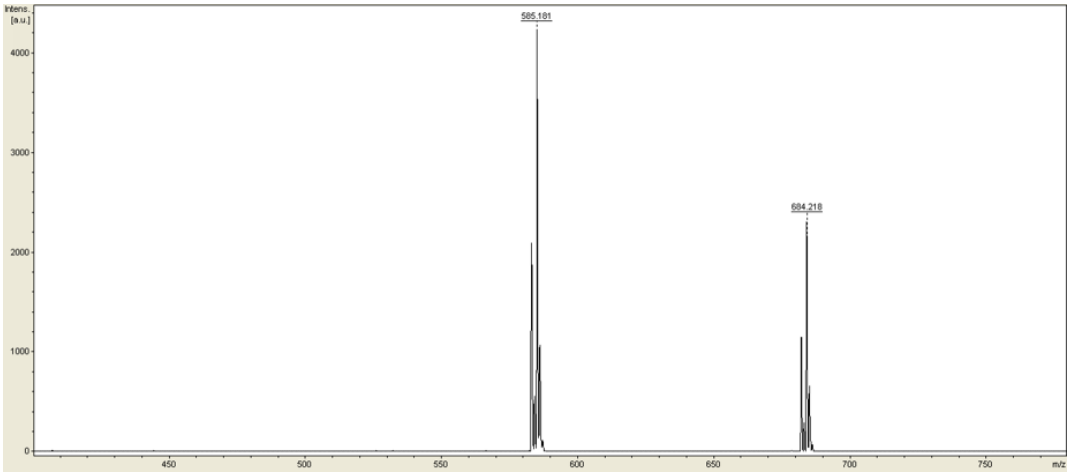

Figure S5. MALDI–TOF data of **1**.

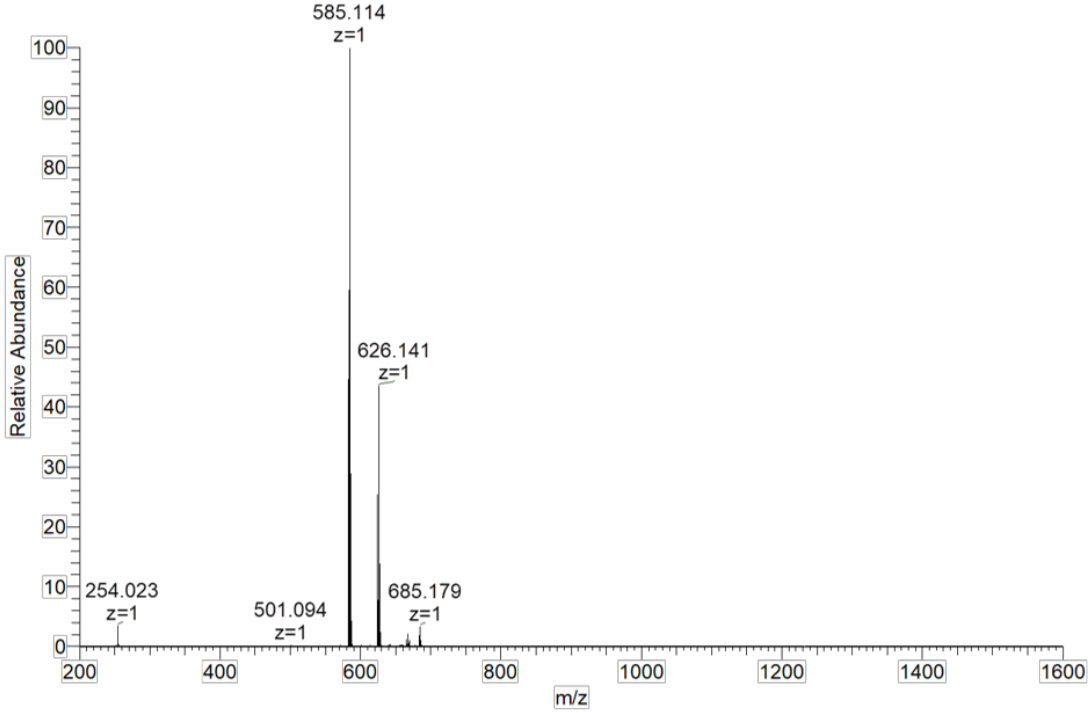

Figure S6. ESI–MS spectra of **1** after the addition of Hg^{2+} ion.

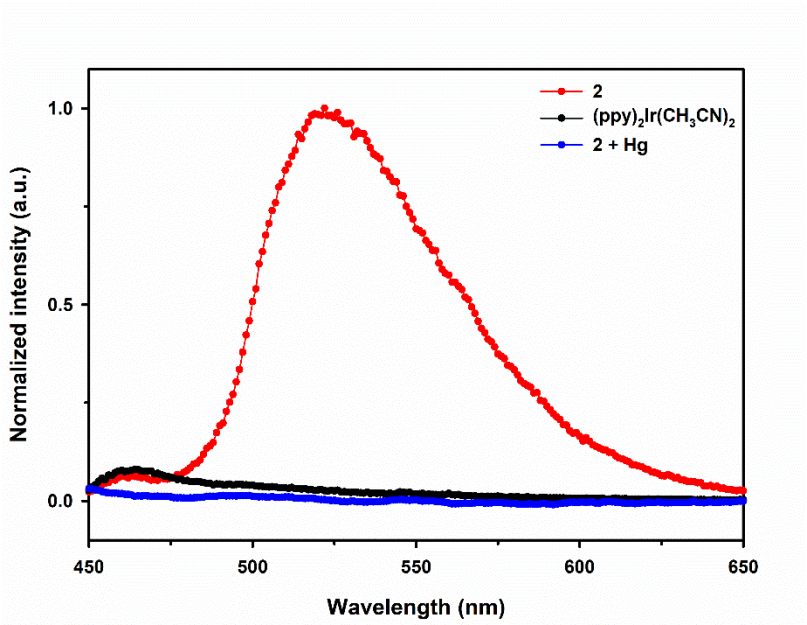

Figure S7. Normalized phosphorescence intensities of **2**, **2** upon the addition of 50 μM Hg^{2+} ion, and $(ppy)_2Ir(CH_3CN)_2$.

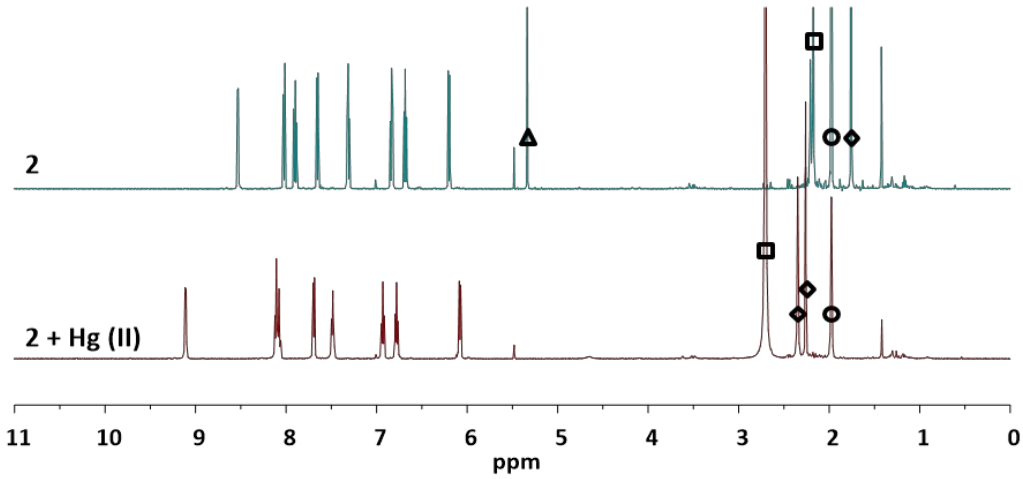

Figure S8. NMR spectra of **2** before and after the addition of Hg^{2+} ion (5 equivalents) in CD_3CN. ○: acetonitrile, □: water, △: H_a, ◇: H_b

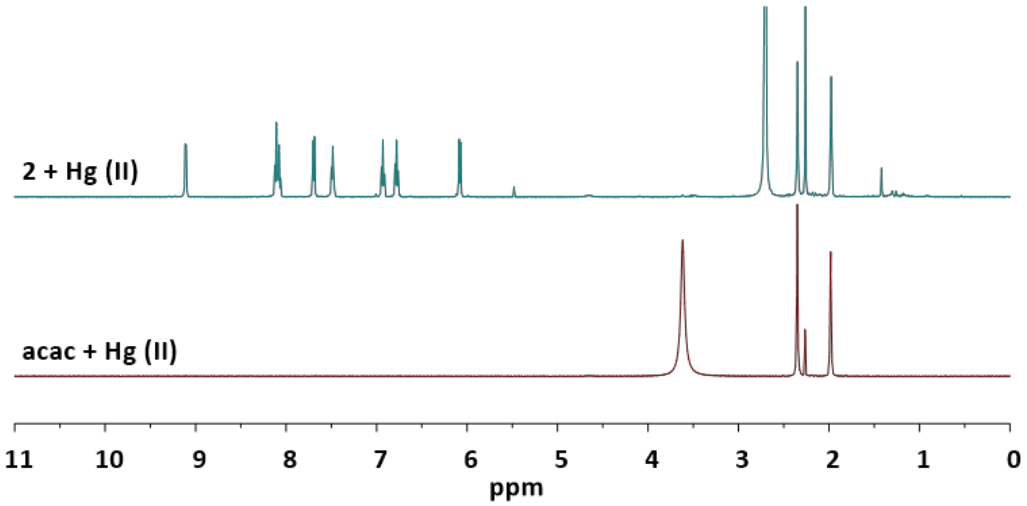

Figure S9. Comparison of NMR spectra of **2** and acetylacetone in the presence of 5 equivalents of Hg^{2+} ion.

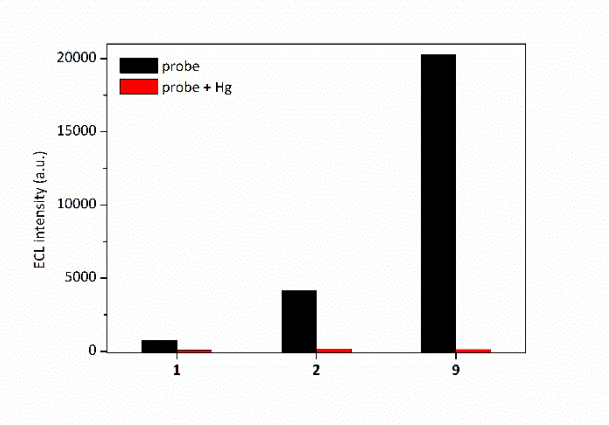

Figure S10. Comparison of ECL intensity of **1**, **2** and **9** before and after the addition of Hg^{2+} ion (80 μM) in CH_3CN/water (9/1).

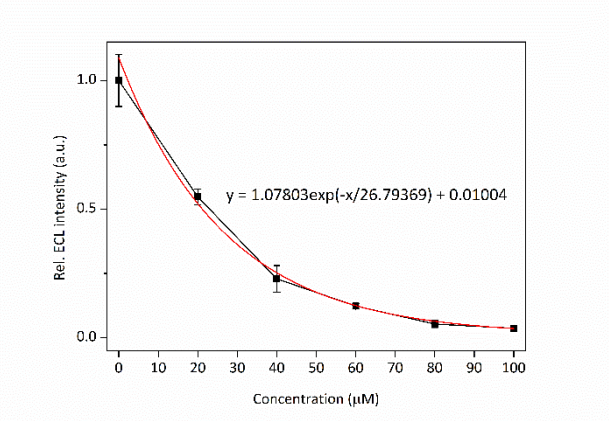

Figure S11. ECL intensity of 10 μM of **1** upon addition of Hg^{2+} ion (0–100 μM) in CH_3CN/water (9/1) (100 mM TPA, and 0.1 M TBAP as the supporting electrolyte). The potential was swept at a Pt disk electrode (diameter: 2 mm) over the range 0–1.8 V vs Ag/AgCl (scan rate: 0.1 V/s). LOD = 1.9 nM.

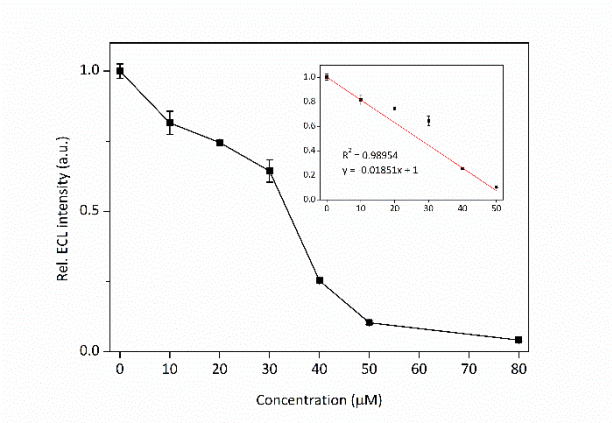

Figure S12. ECL intensity of 10 μM of **2** upon the addition of Hg^{2+} ion (0–80 μM) in CH_3CN/water (9/1) (30 mM TPA, and 0.1 M TBAP as the supporting electrolyte). The potential was swept at a Pt disk electrode (diameter: 2 mm) over the range 0–1.4 V vs Ag/AgCl (scan rate: 0.1 V/s). Inset: Plot of ECL intensity vs [Hg^{2+}] (0–50 μM) showing the linear relationship. LOD = 0.78 nM.

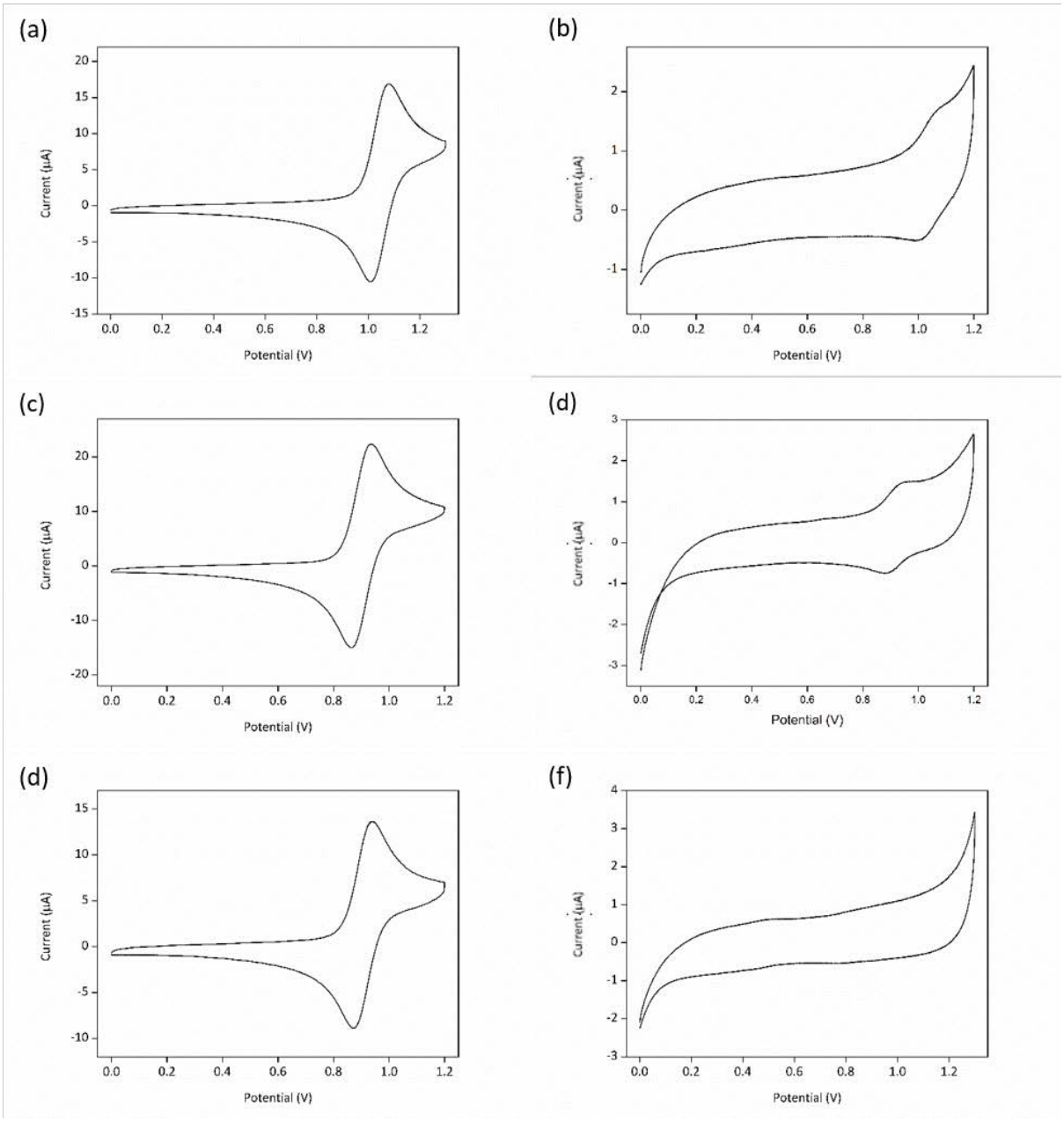

Figure S13. Cyclic voltammograms of (a) **1**, (b) **1** + Hg^{2+} (1 equivalent), (c) **2**, (d) **2** + Hg^{2+} (1 equivalent), (e) **9**, (f) **9** + Hg^{2+} (1 equivalent) in CH_3CN.

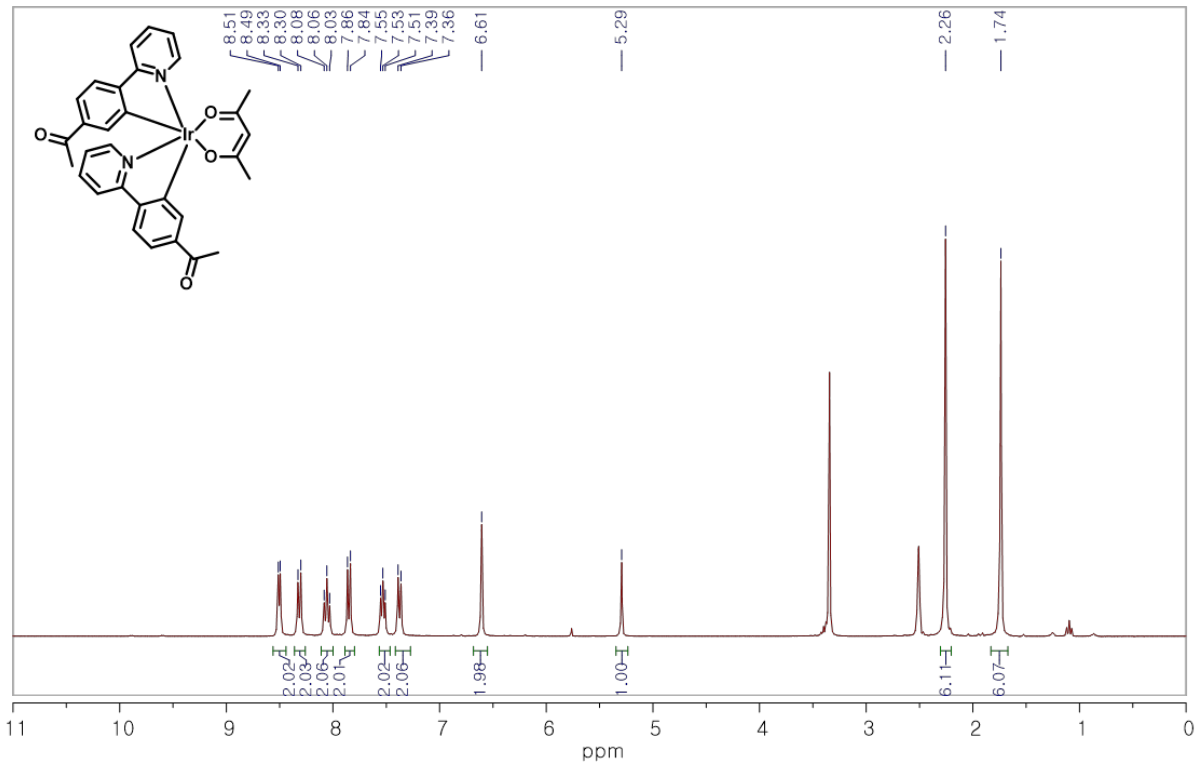

Figure S14. ^{1}H NMR spectrum of **1** (300 MHz, DMSO-d_6).

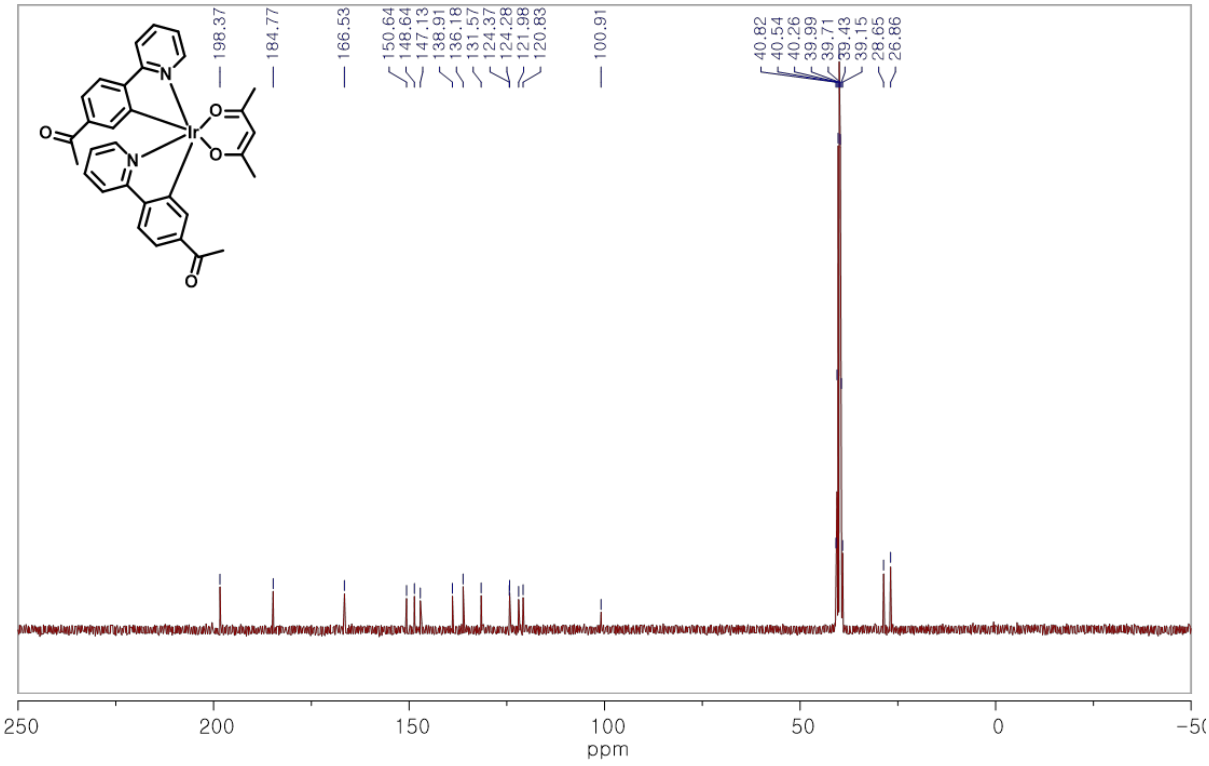

Figure S15. ^{13}C NMR spectrum of **1** (75 MHz, DMSO-d_6).

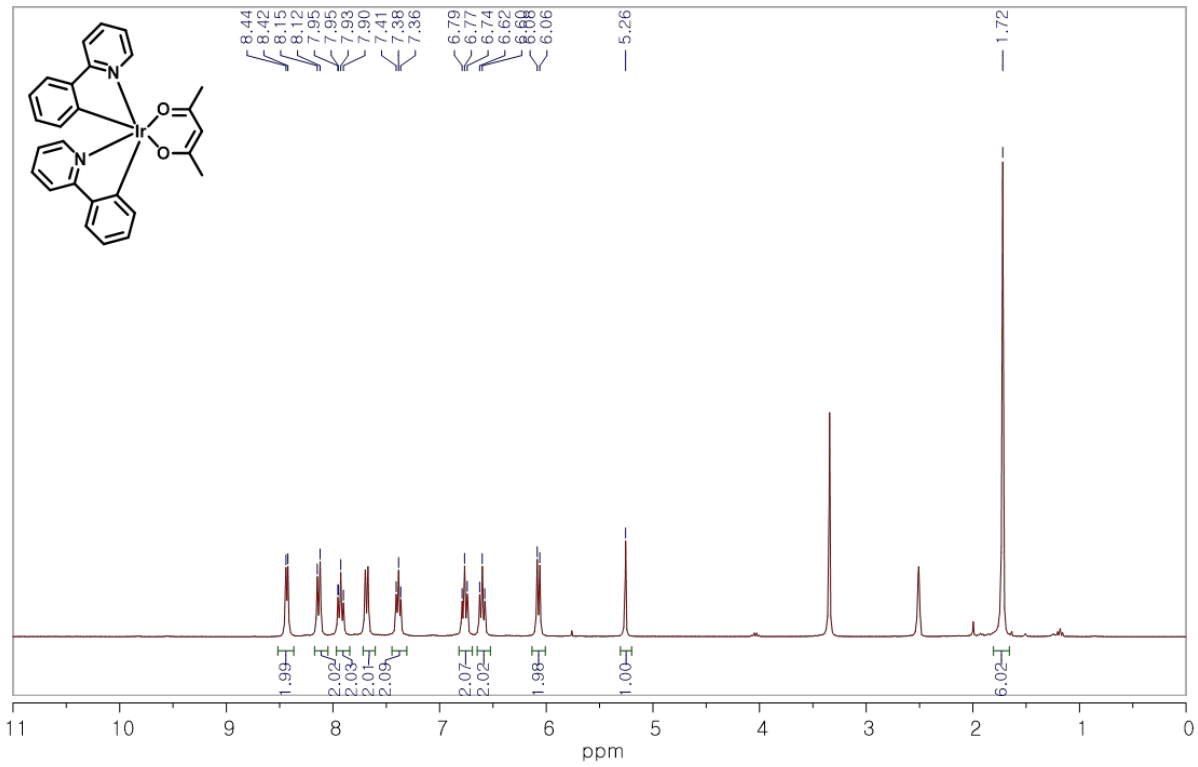

Figure S16. ^{1}H NMR spectrum of **2** (300 MHz, DMSO-d_6).

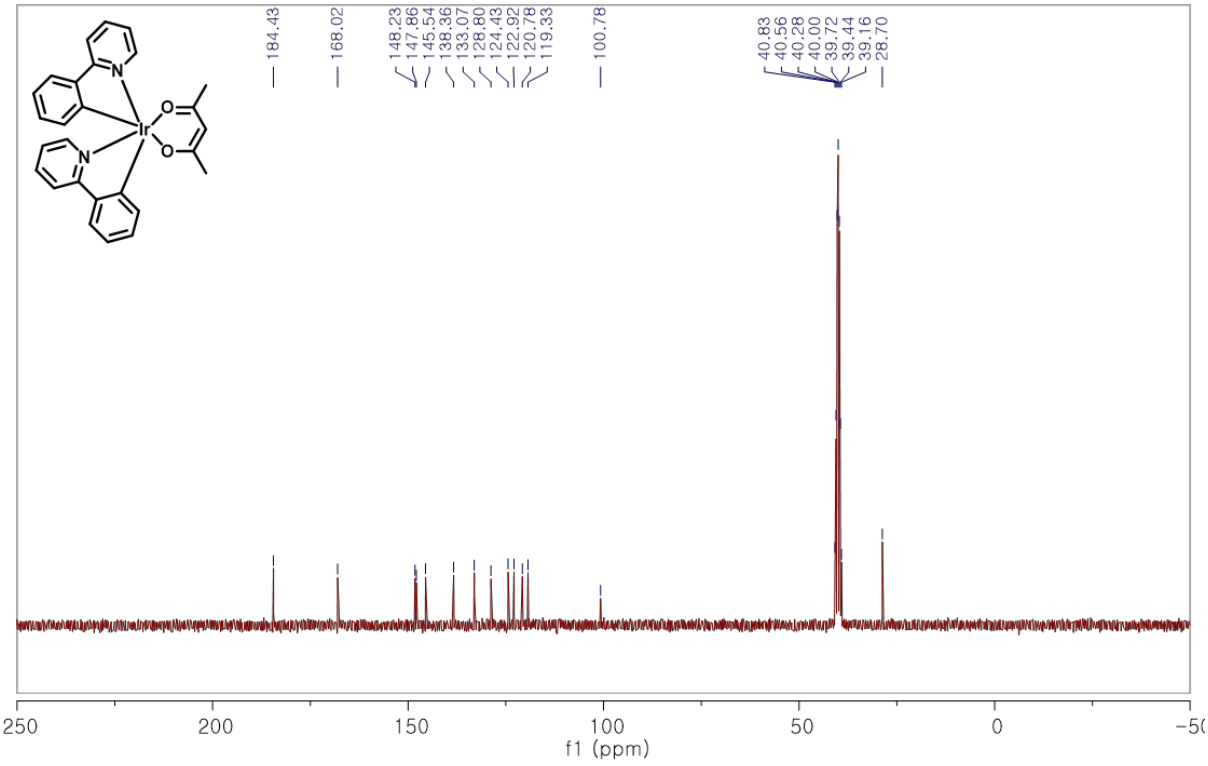

Figure S17. ^{13}C NMR spectrum of **2** (75 MHz, DMSO-d_6).

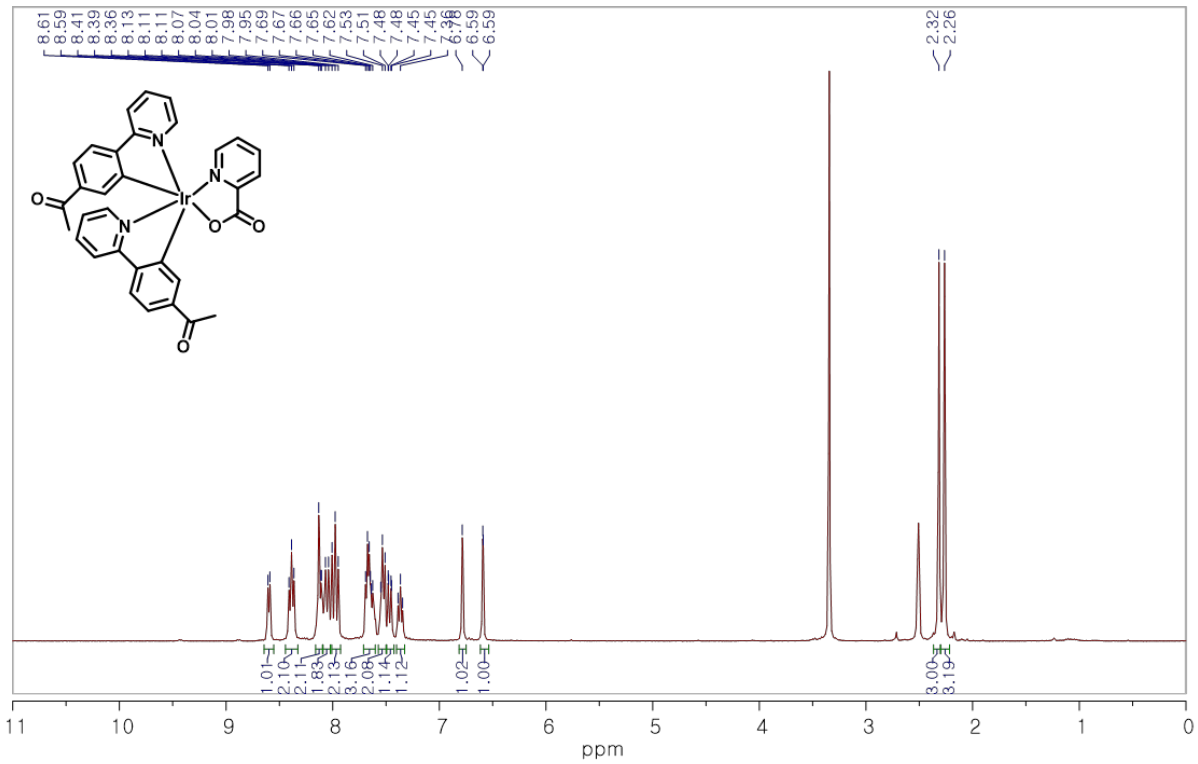

Figure S18. ^{1}H NMR spectrum of **3** (300 MHz, DMSO-d_6).

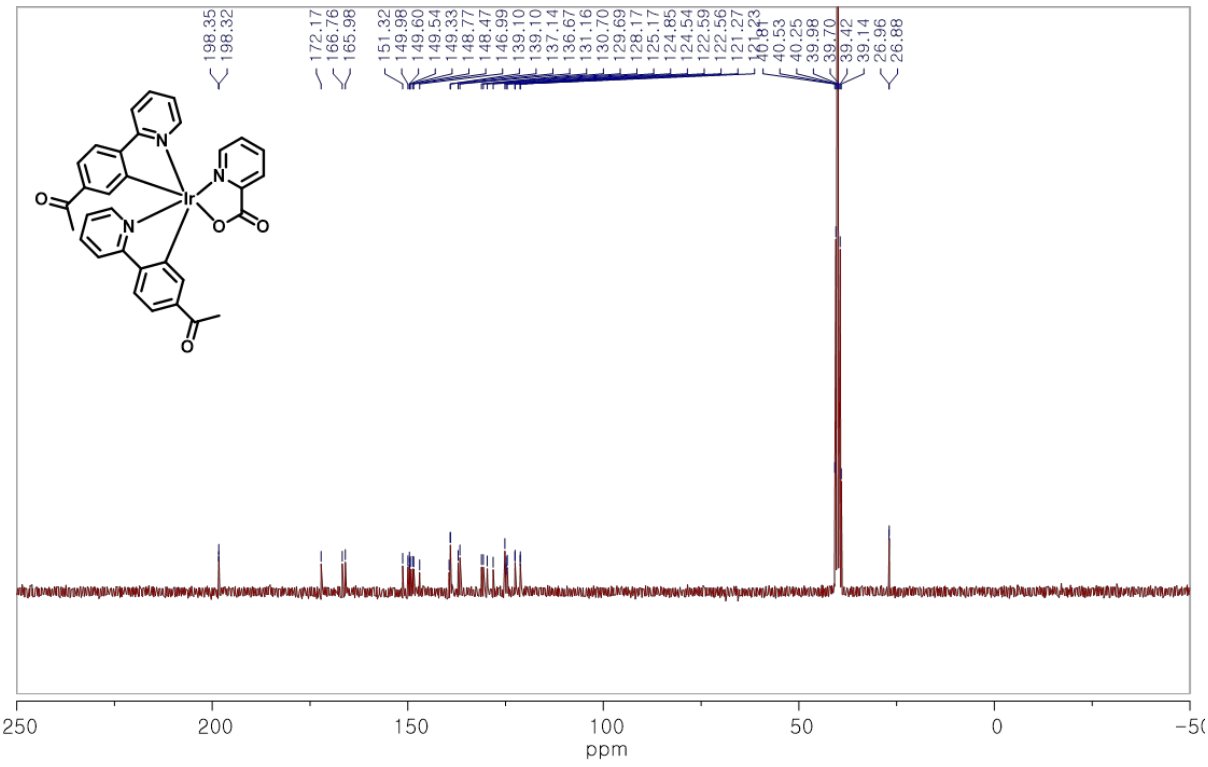

Figure S19. ^{13}C NMR spectrum of **3** (75 MHz, DMSO-d_6).

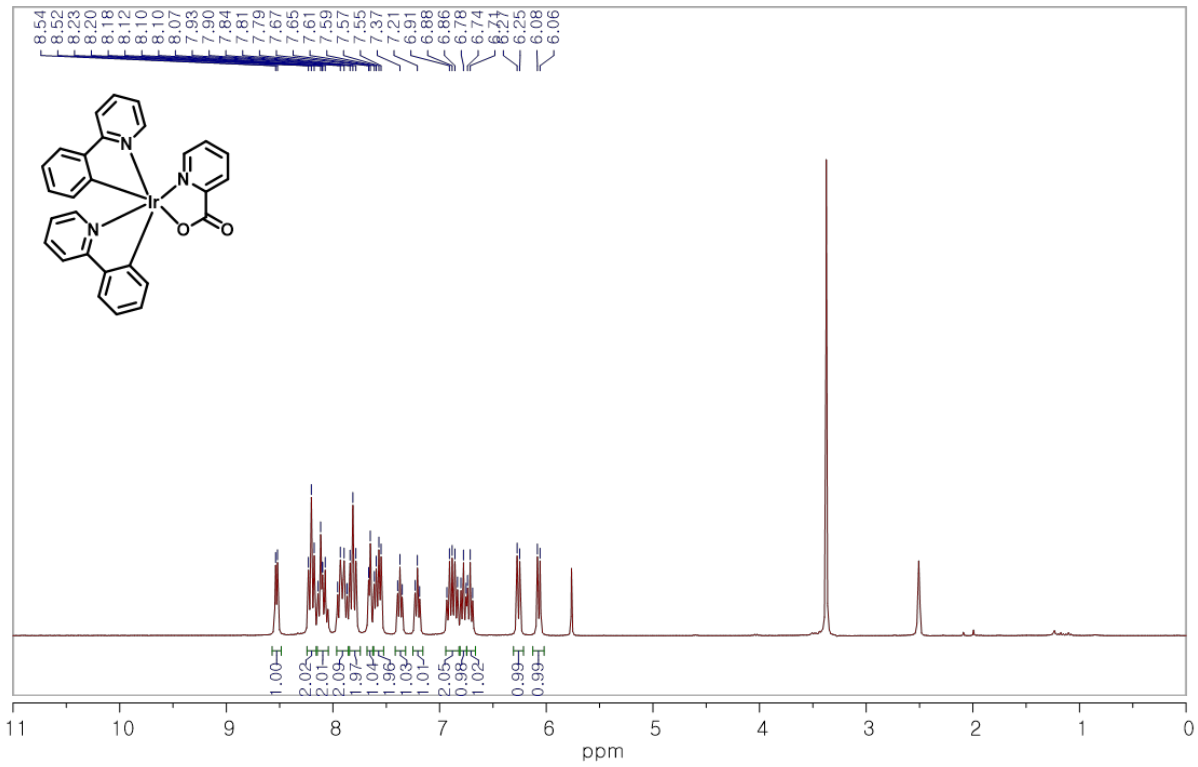

Figure S20. ^{1}H NMR spectrum of **4** (300 MHz, DMSO-d_6).

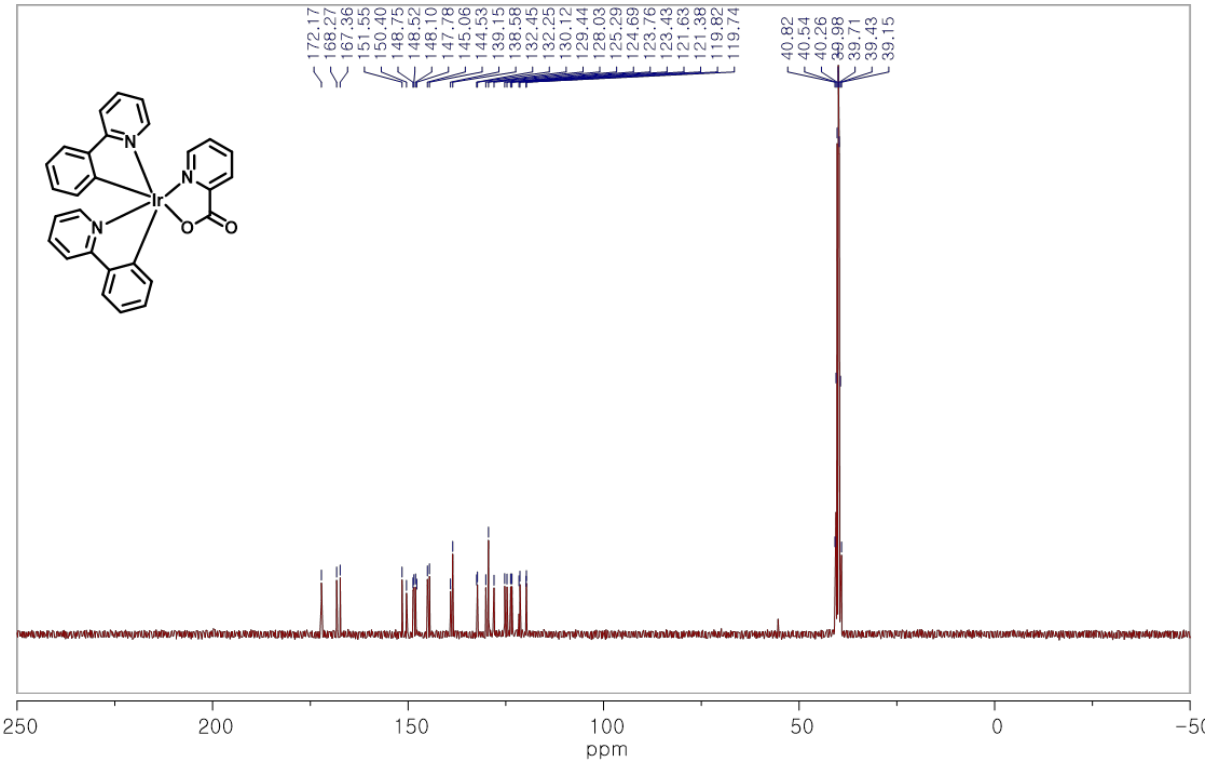

Figure S21. ^{13}C NMR spectrum of **4** (75 MHz, DMSO-d_6).

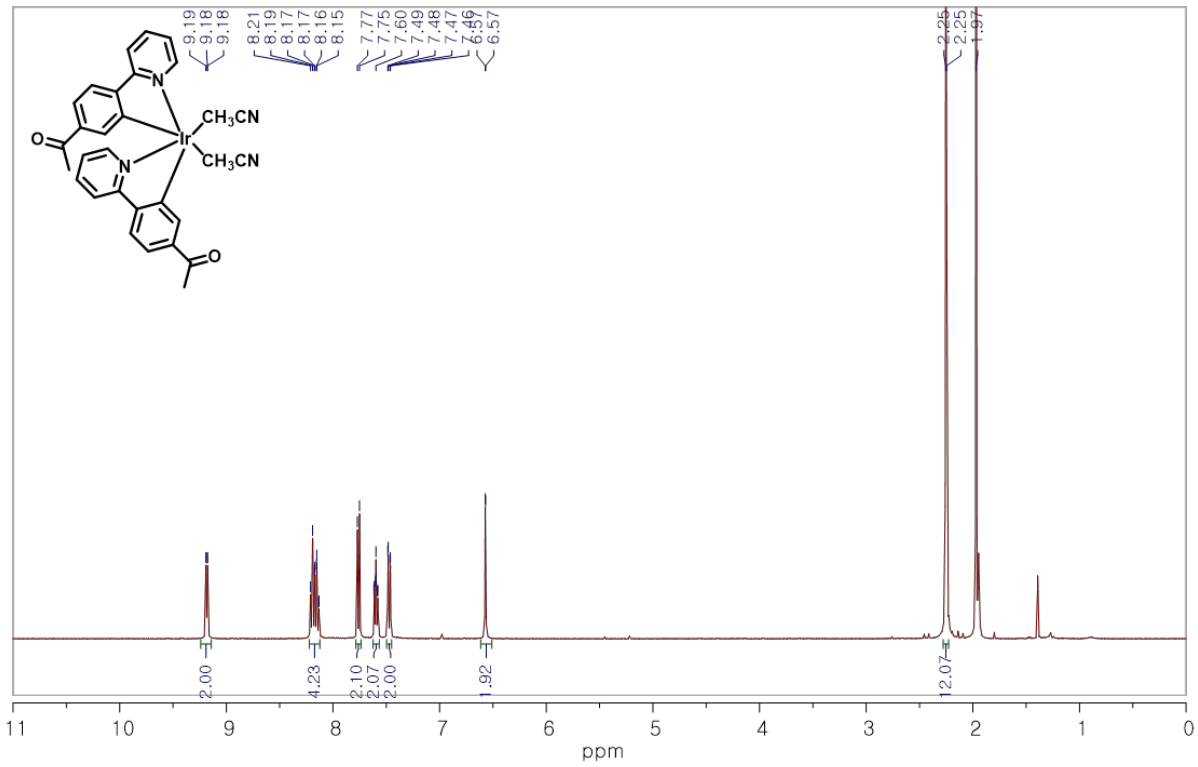

Figure S22. ^{1}H NMR spectrum of **5** (400 MHz, CD_3CN).

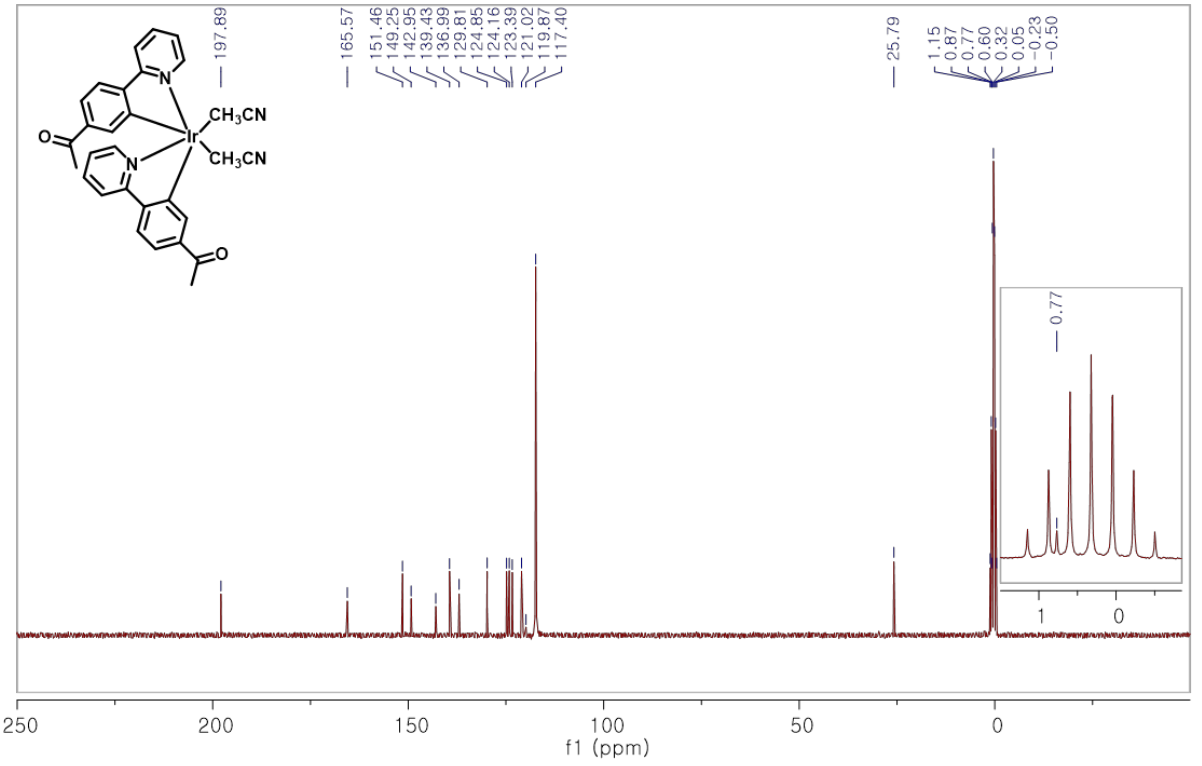

Figure S23. ^{13}C NMR spectrum of **5** (75 MHz, CD_3CN).

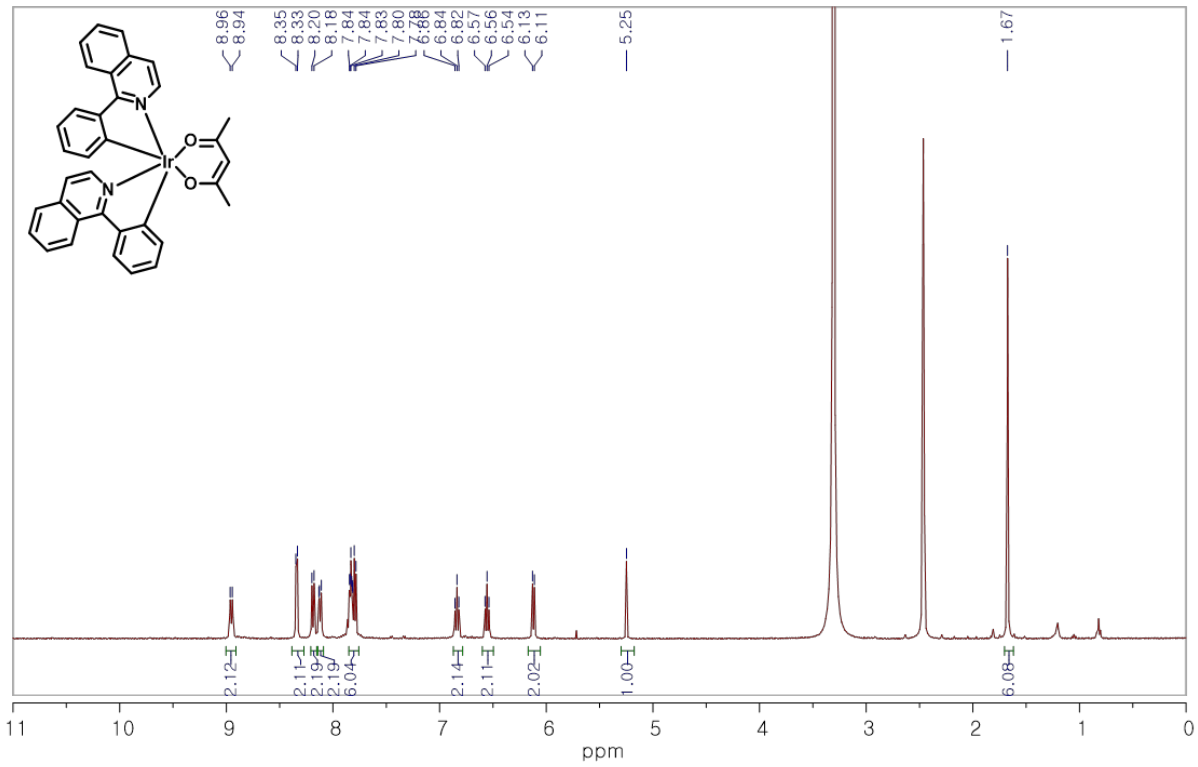

Figure S24. ^{1}H NMR spectrum of **9** (400 MHz, DMSO-d_6).